

Direct detection of pyridine formation by the reaction of CH (CD) with pyrrole: a ring expansion reaction

Satchin Soorkia^a, Craig A. Taatjes^b, David L. Osborn^b, Talitha M. Selby^c, Adam J. Trevitt^d,
Kevin R. Wilson^e and Stephen R. Leone^{a,e,*}

^aDepartments of Chemistry and Physics, University of California, Berkeley, California 94720

^bCombustion Research Facility, Mail Stop 9055, Sandia National Laboratories, Livermore, CA 94551-0969, USA

^cDepartment of Chemistry, University of Wisconsin-Washington County, West Bend, WI 53095

^dSchool of Chemistry, University of Wollongong, New South Wales, Australia

^eChemical Sciences Division, Lawrence Berkeley National Laboratory, 1 Cyclotron Road, Berkeley, CA 94720, USA

*On appointment as a Miller Research Professor in the Miller Institute for Basic Research in Science

Abstract

The reaction of the ground state methylidyne radical CH ($X^2\Pi$) with pyrrole (C_4H_5N) has been studied in a slow flow tube reactor using Multiplexed Photoionization Mass Spectrometry coupled to quasi-continuous tunable VUV synchrotron radiation at room temperature (295 K) and 90 °C (363 K), at 4 Torr (533 Pa). Laser photolysis of bromoform ($CHBr_3$) at 248 nm (KrF excimer laser) is used to produce CH radicals that are free to react with pyrrole molecules in the gaseous mixture. A signal at $m/z = 79$ (C_5H_5N) is identified as the product of the reaction and resolved from ^{79}Br atoms, and the result is consistent with CH addition to pyrrole followed by H-elimination. The Photoionization Efficiency curve unambiguously identifies $m/z = 79$ as pyridine. With deuterated methylidyne radicals (CD), the product mass peak is shifted by +1 mass unit, consistent with the formation of C_5H_4DN and identified as deuterated pyridine (d-pyridine). Within detection limits, there is no evidence that the addition intermediate complex undergoes hydrogen scrambling. The results are consistent with a reaction mechanism that proceeds *via* the direct CH (CD) cycloaddition or insertion into the five-member pyrrole ring, giving rise to ring expansion, followed by H atom elimination from the nitrogen atom in the intermediate to form the resonance stabilized pyridine (d-pyridine) molecule. Implications to interstellar chemistry and planetary atmospheres, in particular Titan, as well as in gas-phase combustion processes, are discussed.

1. Introduction

The methyldyne radical (CH) is one of the most reactive hydrocarbon radical species and plays an important role in combustion chemistry,^{1, 2} the interstellar medium³ and the photochemistry of planetary atmospheres, in particular on Titan, one of Saturn's moons.⁴ The extreme reactivity arises from one singly occupied and one vacant non-bonding molecular orbital localized on the carbon atom.⁵ Rate constants for the reaction of CH with numerous hydrocarbons ranging from methane (CH₄)^{6,7} and acetylene (C₂H₂)⁷ to much larger Polycyclic Aromatic Hydrocarbons (PAHs) like anthracene (C₁₄H₁₀) have been measured.⁸ With small unsaturated hydrocarbons, the reaction proceeds by either direct CH insertion or addition followed by elimination of one H atom from the intermediate adduct.^{5,9,10} Recently Goulay and coworkers⁵ measured isomeric branching fractions in the reactions of CH with several unsaturated hydrocarbons. In general, reactions involving the CH radical are fast, barrierless¹¹ and occur with high exothermicity.⁷

Pyrrole (C₄H₅N) and pyridine (C₅H₅N) are both fundamental 5- and 6-membered heterocyclic molecules (see structures in Figure 1). Both pyrrole and pyridine are important biomolecular building blocks. These N-containing molecules and their derivatives are essential for vital biological functions. In astrobiology, it is believed that organic ring compounds, including N-heterocycles, could have played an important role in the co-evolution of life and planetary environments in prebiotic chemistry.¹² In that respect, Titan, the intriguing satellite of the Solar system with a substantial atmosphere composed of mainly molecular nitrogen (N₂) and methane (CH₄), is a captivating object to the scientific community. Indeed, its organic-rich (both hydrocarbons and nitriles), low-temperature atmosphere and photoactive haze present many analogies with the primitive Earth.¹³ In attempts to simulate Titan tholin and prebiotic chemistry in laboratory experiments,^{14,15} pyrrole and pyridine have been identified¹⁶ as key molecules in addition to other molecular species including N-containing polycyclic aromatic compounds.

Nevertheless, the respective (bio)chemical functions of pyrrole and pyridine may be profoundly different due to their intrinsic structural difference. Pyridine is structurally close to benzene (C₆H₆) where a CH group has been replaced by a N atom (see structures in Figure 1), and yet it

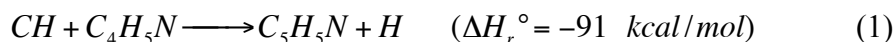
exhibits a different reactivity compared to its homocyclic counterpart. At a minimum, pyridine has a net dipole moment ($\mu_D = 2.19$ Debye)¹² compared to benzene, which has no net dipole moment, and therefore could interact differently with polar and charged compounds. Both pyrrole and pyridine follow Hückel's rule and therefore have aromatic properties. However, the lone pair of electrons on the nitrogen atom in pyridine is not delocalized in the aromatic ring as they are in pyrrole. This difference accounts for the basicity of pyridine with chemical properties often close to tertiary amines. With the availability of the lone pair electrons, pyridine can act as a N-nucleophile or ligand without disrupting the resonance stabilization conferred by aromaticity.

In devising more elaborate photochemical models^{4,17,18} to understand the complex nature of Titan's atmosphere, accurate experimental data is vital.⁴ Both kinetic measurements and accurate product identification including branching ratios are integral to reliably assess the role and importance of hydrocarbon and nitrile species in the evolution of Titan's atmosphere. Pyrrole and pyridine provide archetypal examples of how fundamental physical and chemical properties could be significantly different for two cyclic molecules that differ by only one carbon atom. Key small N-heterocyclic species like pyrrole and pyridine are among those that are likely to be important. Reactions of these molecules with radical and/or ionic species subsequently could give rise to larger nitrogen containing carbonaceous species. Ricca and coworkers¹⁹ have shown that inclusion of a nitrogen atom into a PAH could promote the formation of additional hydrocarbon rings by lowering the ring closing barrier. Ultimately, these molecules could contribute to the formation of much larger Polycyclic Aromatic Nitrogen Heterocycles (PANHs) that are believed to play an important role in interstellar chemistry.

Furthermore, both pyrrole and pyridine are important sources of the so-called "fuel nitrogen" in processes leading to the combustion-generated air pollutant, nitric oxide (NO), from coal and coal-derived fuels.¹ Typically, coal contains 0.5 – 2.5% of nitrogen by weight,²⁰ most of which occurs as heterocyclic aromatic rings or ring clusters, i.e. stored in pyrrolic and pyridinic structures.²¹ In understanding the mechanisms and modeling of combustion processes, in particular for nitrogen containing molecules, it is necessary to have a detailed knowledge of the reactivity of such heterocyclic molecules with other species, e.g. CH radicals, in the gas-phase. In addition, N-containing aromatic molecules, for the same reason stated in the paragraph above,

could also contribute to molecular weight growth, leading to the formation of soot particles in combustion flames.

In this paper, we report the direct product detection of the gas-phase reaction of the CH radical with pyrrole as shown in Eq. 1 below (1 kcal = 4.184 kJ):



The reaction has been studied at room temperature (295 K) and 90 °C (363 K) in a slow flow tube reactor using Multiplexed Photoionization Mass Spectrometry (MPIMS) coupled to the quasi-continuous tunable VUV synchrotron radiation (Chemical Dynamics Beamline) at the Advanced Light Source (ALS) at the Lawrence Berkeley National Laboratory (LBNL). The time-resolved Photoionization Efficiency (PIE) curve, i.e. the ion signal as a function of the synchrotron photon energy, of $m/z = 79$ (C_5H_5N) unambiguously identifies the product of the reaction as pyridine. In the case of $CD + C_4H_5N$, we detect essentially no C_5H_5N and conclude that the H atom lost always comes from the N atom in pyrrole. The N-H bond in pyrrole is weaker than any of the C-H bonds in pyrrole, providing a thermodynamic driving force for this selective outcome and the lack of randomization of the H atoms in the adduct. The possible generality of such ring expansion reactions in combustion will be important to characterize. The implications of the experimental results for the photochemistry of the interstellar medium and the atmosphere of Titan are also indicated.

2. Experimental Apparatus

The CH (CD) + pyrrole (C_4H_5N) reaction has been studied in a slow flow reactor coupled to tunable VUV synchrotron radiation at LBNL.²² The experimental setup,²² inspired by the general PIMS design of Slagle and Gutman,²³ has been described in previous studies²⁴⁻²⁶ and only a brief overview will be given here. Typically, the gas flow consists of small amounts of the radical precursor ($CHBr_3$, $2.0 \times 10^{13} \text{ cm}^{-3}$) and the reactant (pyrrole, $5.0 \times 10^{14} \text{ cm}^{-3}$) in helium carrier gas. A small amount of N_2 is added to the main flow to quench any vibrationally excited CH radicals.⁵ All flows are metered using calibrated mass flow controllers. The pressure inside the

flow tube is maintained at 4 Torr (533.3 Pa) by adjusting the pumping speed of the Roots blower using a butterfly valve. At this pressure and room temperature, the total density inside the flow reactor is typically $1.3 \times 10^{17} \text{ cm}^{-3}$.

The reaction is initiated by the pulsed laser photolysis (PLP) technique. The reactor is a 62 cm long quartz tube with a 1.05 cm inner diameter, wrapped with nichrome heating tape. An unfocused 248 nm laser beam propagates down the axis of the reactor, generating an initial uniform concentration of CH radicals along the tube. Bromoform (CHBr_3) is used as the radical precursor. It has been shown that CHBr_3 photodissociation occurs *via* successive absorptions of several photons at 248 nm at a fairly low photon density, as opposed to multiphoton absorption.²⁷ In our experiment, the photolysis fluence is typically $\sim 15 \text{ mJ/cm}^2$ in a $\sim 20 \text{ ns}$ pulse duration inside the flow tube. The repetition rate of the laser is 4 Hz in our experiment, and the flow velocity inside the reactor is kept constant at $\sim 8 \text{ m/s}$ to ensure the photolysis of a fresh gas mixture for each laser pulse.

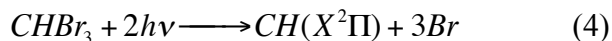
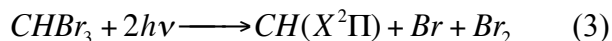
Neutral species escape from a $650 \text{ }\mu\text{m}$ diameter pinhole on the side of the quartz tube forming an effusive beam that is skimmed by a 0.15 cm diameter skimmer and crossed by the VUV synchrotron radiation at the Chemical Dynamics Beamline at the ALS. The quasi-continuous and tunable radiation may, if sufficiently energetic, ionize the species inside the molecular beam. The ions created are then monitored simultaneously using orthogonal-acceleration time-of-flight mass spectrometry and a micro-channel plate detector. Typically for each photon energy, the experiment is repeated for 200-250 laser pulses and the collected data are summed. Time-dependent, multiplexed mass spectra are recorded as a function of the synchrotron photon energy (9.0-10.2 eV energy range). Thus, the collected data sets are 3-dimensional (3D) time- and energy-resolved mass spectra.²²

The purities of the gases are as follows: He 99.9999%, CDBr_3 99.5 %, CHBr_3 99.5 % and pyrrole 99%. Commercial pyrrole was purified by distillation prior to the experiments. A pure sample of pyrrole is transparent after removal of impurities, mainly polypyrrole that is responsible for the yellow-orange color. The CDBr_3 and CHBr_3 are degassed by several freeze-pump-thaw cycles before use.

3. Results

At 248 nm, the reported cross section of pyrrole²⁸ is $3.9 \times 10^{-20} \text{ cm}^2$. The photoionization and photodissociation dynamics of pyrrole have been studied by Ashfold and coworkers²⁹ using photoelectron imaging and ion time-of-flight mass spectrometry. It is shown that fragmentation of pyrrole at 243 nm occurs via a multiphoton process and mass peaks corresponding to H^+ , C^+ , C_2^+ , CNH_2^+ , C_3^+ , C_3H_3^+ and $\text{C}_4\text{H}_5\text{N}^+$ ions are detected. In comparison, the photolysis laser in the current study is an unfocussed beam at 248 nm. We estimate our photolysis intensity (W/cm^2) is at least a factor of 100 smaller. Multiphoton processes are therefore not expected, which is confirmed by the absence of $m/z = 39$ (C_3H_3 , IE = 8.67 eV). Therefore contributions of side reactions of photoproducts to the ion signal of interest are neglected.

At room temperature, the absorption cross-section of bromoform²⁷ at 248 nm is $1.94 \times 10^{-18} \text{ cm}^2$. Bromoform is known to be an efficient precursor of CH radicals along with brominated fragments. A recent cavity ring-down absorption spectroscopy (CRDS) study³⁰ quantified the CH production efficiency $\Phi = N(\text{CH})/N(\text{CHBr}_3) = 5(\pm 2.5) \times 10^{-4}$ at 248 nm with a photolysis laser fluence of $44 \text{ mJ}/\text{cm}^2$ per pulse, corresponding to a two-photon process only. At a single photon of 248 nm, the triplet states of CHBr_3 are accessible and two dissociation channels for further CH production are relevant,³⁰ i.e. $\text{CHBr}_2 + \text{Br}$ and $\text{CHBr} + \text{Br}_2$. At 248 nm two-photon absorption, three new dissociation channels are accessible as described³⁰ and indicated in Eq. 2 to 4 below:



Production of excited CH ($\text{A}^2\Delta$) state is not accessible by two-photon excitation and requires at least three photons at 248 nm.³⁰ The successive photodissociation scheme of CHBr_3 outlined above indicates that careful adjustment of the laser fluence is critical to produce preferentially CH ($\text{X}^2\Pi$) while minimizing CH ($\text{A}^2\Delta$). The photodissociation leaves behind Br_2 molecules and radical species (CHBr , CHBr_2 , Br) that might react with pyrrole to form stable products.

However, these product masses are expected to be at much higher molecular weight compared to the expected product channel of the title reaction, i.e. C_5H_5N (79.04 amu) or C_5H_4DN (80.05 amu). In addition, the well-known relative isotopic abundances of ^{79}Br and ^{81}Br , i.e. 50.7% and 49.3% respectively, serve to identify or rule out brominated products.

Dissociative ionization of the brominated species could also contribute to the ion signal at lower masses.⁵ To our knowledge, kinetic data on the reactions of brominated radical species with pyrrole are unavailable. But, the reaction rate coefficients of the bromomethylidyne radical (CBr) with alkenes and alkynes at room temperature have been measured and found to be much smaller ($< 10^{-12} \text{ cm}^3 \text{ molecule}^{-1} \text{ s}^{-1}$)³¹⁻³³ than for analogous reactions with CH radical ($\sim 10^{-10} \text{ cm}^3 \text{ molecule}^{-1} \text{ s}^{-1}$).^{34,35} Based on these observations, it is reasonable to assume that the reaction of CBr with pyrrole is at least 100 times slower than the CH with pyrrole reaction. Given our instrumental time resolution, the kinetic evolution of products from CBr with pyrrole could easily be resolved. Careful comparison of the time profiles of higher-mass species to $m/z = 79$ ion signal suggests that the contribution from dissociative ionization is negligible.

Below, we present the results for the reaction of CH with pyrrole at room temperature (295 K) and 90 °C (363 K) at 4 Torr (533 Pa). The reactions are also studied with CD radicals in order to shed light on the mechanism of the reaction.

3.1. $CH + C_4H_5N \rightarrow \text{pyridine} + H$

Figure 2(a) shows a mass spectrum at a photoionization photon energy of 10.2 eV resulting from the reaction of CH with pyrrole at 363 K. The largest peak is observed at $m/z = 79$, consistent with the H-loss channel of the reaction leading to the formation of C_5H_5N . Figure 3 is a time-resolved mass spectrum of the reaction at 10.2 eV at 90 °C (363 K). Pyrrole ($m/z = 67$) and the reaction product C_5H_5N ($m/z = 79$) are apparent. Note that both the time traces and ion intensities show that $m/z = 68$ and 80 are the $M+1$ mass peaks relative to the main peaks, M , due to the natural abundance of ^{13}C atoms. The time evolution of the intensity of $m/z = 79$ for both room temperature (295 K) and 363 K are shown in Figure 4. The time profiles are shown without background subtraction, i.e. without subtracting the contribution of the pre-laser signal to $m/z = 79$. The product is clearly distinguished because it appears immediately after the laser pulse at $t =$

0 ms (indicated by a dashed line in Figure 3 and sharp rise time in Figure 4(a) and (b)), and remains constant within the reaction time as shown in Figure 4(b), at least for $0 < t < 30$ ms.

Comparing the $m/z = 79$ signals in Figure 4(a) and (b), heating the flow tube improves the signal-to-background ratio by a factor of ~ 3 from 295 K to 363 K. The time profile of the signal shown in Figure 4(b) is consistent with the heating profile of the tube, i.e. 39 cm of the tube is heated, beginning 23 cm above the pinhole. For a flow velocity of $\sim 8 \text{ ms}^{-1}$, this length of heated gas takes ~ 30 ms to traverse the pinhole. As seen in Figure 4(b), the signal starts to drop around $t = \sim 30$ ms, which reveals that photolyzed gas from the unheated section of the tube is sampled at later times. As identified in the paragraph below, $m/z = 79$ is pyridine. At room temperature, some pyridine molecules formed in the title reaction may diffuse radially and adsorb to the wall of the tube, explaining the drop in the signal in Figure 4(a) after initial pyridine formation when the laser is pulsed at $t = 0$. A substantial amount of pyridine from subsequent desorption remains in the flow before each laser photolysis pulse, explaining the relatively prominent pre-laser background for $t < 0$. Heating the tube reduces the adsorptive removal, as shown by the relatively stable $m/z = 79$ signal over the ~ 30 ms transit time of the heated sample in Figure 4(b), and the smaller total adsorption results in a concomitantly smaller pre-laser signal from desorbing pyridine.

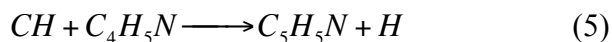
Figure 5(a) shows an energy-resolved mass spectrum of the title reaction at 363 K. The $m/z = 79$ ion signal is integrated for $0 < t < 50$ ms as a function of the synchrotron photon energy to obtain the Photoionization Efficiency (PIE) curve shown in Figure 5(c). The threshold in the ion signal is observed around 9.25 eV. The signal then rises slowly in the 9.25 - 9.5 eV range and then almost linearly above 9.5 eV as a function of photon energy. This threshold corresponds to the value of the ionization energy of pyridine found in the literature ($IE = 9.26 \pm 0.01 \text{ eV}$).³⁶ Moreover, the signal can be fit using a relative PIE curve for pyridine, acquired from a known pure sample, as shown by the black curve in Figure 5(c). Since no additional thresholds are observed in the ion signal between 9.0 - 10.2 eV, we conclude that the only isomer produced from the title reaction is pyridine.

3.2. $\text{CD} + \text{C}_4\text{H}_5\text{N} \rightarrow \text{d-pyridine} + \text{H}$

Figure 2(b) shows a mass spectrum for the reaction of deuterated methylidyne (CD) with pyrrole. In comparison with Figure 2(a), showing the mass spectrum for the reaction of CH with pyrrole, it can be noted that the product mass peak is almost entirely shifted by +1 mass unit as well as the ^{13}C -derived $M + 1$ mass peak. It is notable that $m/z = 79$ ($\text{C}_5\text{H}_5\text{N}$) ion signal is almost negligible (3.5%) and most probably originates from a small contamination of the hydrogenated species in CDBr_3 sample (isotopic purity of 99.5 atom % D, Sigma Aldrich). The results are consistent with the formation of $\text{C}_5\text{H}_4\text{DN}$. As discussed below, we interpret this observation to mean that the hydrogen atom that is lost following CH addition is always the H atom bound to the N atom in the pyrrole reactant. Figure 5(a) and (b) show a comparison of the photoionization energy-resolved mass spectra between the reactions with CH and CD. It can be seen that both products have identical photoionization efficiency spectra identifying the $m/z = 80$ ion signal d-pyridine as shown in Figure 5(d). Similarly to the nondeuterated reaction, d-pyridine is the sole isomeric product of $\text{CD} + \text{pyrrole}$.

4. Discussion

We have presented the direct identification of a ring expansion reaction involving the CH radical with the N-heterocyclic ring molecule, pyrrole. Our results demonstrate the addition of a carbon atom into the pyrrole ring, followed by hydrogen elimination, to form the resonance stabilized 6-membered ring molecule, pyridine. Moreover, the deuterated results suggest that a D atom is exclusively incorporated into the pyridine ring for the reaction of CD with pyrrole. In the first part of this section, we discuss the possible mechanism³⁷ for the reaction based on the experimental results, which can be summarized with Eqs. 5 and 6 below:



where $\text{C}_5\text{H}_5\text{N}$ is pyridine and $\text{C}_5\text{H}_4\text{DN}$ is d-pyridine. In the second part, we discuss possible implications for interstellar chemistry and planetary atmospheres, in particular Titan, as well as combustion chemistry.

4.1. Ring expansion reaction mechanism

At low temperatures, reactions of carbon containing radicals (e.g. C, CH, CH₂ and CN)^{34, 38-43} with unsaturated hydrocarbon species are commonly expected to proceed *via* the formation of an initial short-lived intermediate, formed with almost no entrance barrier. These intermediates subsequently undergo rapid decomposition, often *via* H atom elimination, to give the substituted products. Recently, Goulay and coworkers⁵ studied the reaction between the CH radical and small unsaturated hydrocarbons, namely ethylene (C₂H₄), acetylene (C₂H₂), allene (CH₂CCH₂), and methylacetylene (CHCCH₃), and examined the formation of cyclic versus linear product isomers. Typically, the reactions proceed by either CH insertion or addition followed by H atom elimination from the intermediate adduct.

Berman and coworkers⁴⁴ measured the rate constant for the reaction of CH with aromatic compounds, i.e. benzene (C₆H₆) and toluene (C₆H₅-CH₃). In both cases, they found very large rate constants: $k_{C_6H_6} = (4.3 \pm 0.3) \times 10^{-10} \text{ cm}^3 \text{ molecule}^{-1} \text{ s}^{-1}$ and $k_{C_6H_5-CH_3} = (5.0 \pm 0.4) \times 10^{-10} \text{ cm}^3 \text{ molecule}^{-1} \text{ s}^{-1}$ respectively. As a general conclusion to their kinetic studies, the authors suggest that the reactivity of CH with benzene and toluene is similar to the reactivity of CH with other unsaturated, π -bond containing species.

Low temperature rate coefficients for the reaction of CH with a Polycyclic Aromatic Hydrocarbon (PAH), anthracene, have been measured by Goulay and coworkers⁸ using the well-known Cinétique de Réaction en Ecoulement Supersonique Uniforme (CRESU) technique.^{45,46} The authors conclude that the reaction is barrierless with a slight positive evolution of the rate coefficient with increasing temperature. The reaction is very fast and close to the collision rate. Furthermore, this behavior suggests that a collision-stabilized association process is not involved in contrast to the reaction of OH with anthracene.⁴⁷ It is suggested that the reaction could probably lead to the formation of cyclopropa[b]anthracene assuming that the mechanism proceeds by the addition of the CH radical to the π -system of the molecule followed by a H atom elimination.

To our knowledge, no kinetic data are available for the reaction of the CH radical with pyrrole. Based on the related previous studies, we can assume that the rate coefficient for the reaction of the CH radical with pyrrole is most certainly close to the collision limit, i.e. $k \approx 4 \times 10^{-10} \text{ cm}^3 \text{ molecule}^{-1} \text{ s}^{-1}$. This assumption is supported by the observation of a sharp rise time of the product as seen in Figure 4(c) and (d). Again, because of the temporal resolution of our instrument, it is not possible to measure the bimolecular rate constant for the reactions shown in Eqs. 5 and 6. As discussed by Goulay and coworkers,⁸ it is then reasonable to assume that the mechanism of the title reaction proceeds *via* the addition of the radical to a double bond forming a short-lived intermediate that subsequently decomposes to give the stable product, i.e. pyridine, with the elimination of an H atom.

Moreover, the use of CH and CD radicals in our study provides insight into the reaction mechanism following the formation of the initial adduct. As shown in the mass spectra of Figure 2, the $m/z = 79$ mass peak is shifted by +1 mass unit when CH radicals are replaced by CD radicals in the flow. This result implies that a selective bond rupture likely occurs forming primarily one isotopologue, i.e. d-pyridine at $m/z = 80$. As seen in Figure 1, pyrrole ($\text{C}_4\text{H}_5\text{N}$) has a hydrogen atom attached directly to the nitrogen atom within the heterocyclic ring, while this is not the case with pyridine ($\text{C}_5\text{H}_5\text{N}$). From the CD + pyrrole reaction, which yields exclusively d-pyridine, the mass spectra reveal that the final product retains the D atom within its structure. As a matter of fact, the N-H bond, which is present in the pyrrole structure, needs to be exclusively cleaved in order to form the pyridine ring as the final stable product. As seen in Table 1, the N-H bond is indeed the weakest bond in the pyrrole molecule with a calculated bond dissociation energy (BDE) of 89.8 kcal/mol,⁴⁸ in good agreement with the experimental value of 88 ± 2 kcal/mol. Note that the BDE of the C-H bond in pyridine on site 1 is slightly lower than the BDE on sites 2 and 3 in pyridine, in contrast with the C-H BDEs in pyrrole, which are almost equivalent for sites 1 and 2 (see Figure 1 for labels). Also, the absence of hydrogen randomization supports the fact that selective bond cleavage occurs.

Based upon these considerations, a 4-step mechanism is proposed as depicted in Figure 6. The first step involves the cycloaddition of CH (CD) to one of the double bonds of pyrrole. The second step involves ring expansion leading to the formation of the resonance-stabilized

pyridine-like radical species (C_5H_6N). Subsequently, bond rearrangement followed by rapid decomposition with N-H bond fission, as a final step of the mechanism, leads to the formation of the stable pyridine molecule. Insertion into the single C-C bond of pyrrole is also possible and would lead to the allylic stabilized intermediate, i.e. species 2 and 3 in Figure 6. However, in this experiment we cannot distinguish between cycloaddition and insertion in the pyrrole ring. From the C_5H_6N intermediate, other H-elimination pathways due to the rupture of any of the C-H bonds would lead to the formation of diradical C_5H_5N species. Alternatively, severing the N-H bond leads to the formation of the closed-shell pyridine molecule plus an H atom. It stands to reason that this pyridine-forming channel is the most exothermic and is favored.

An analogy can also be drawn from the study of Thiesemann and coworkers⁴⁹ on the reactions of $CH/CD + C_2H_4$. The small kinetic isotope effect measured and the characterization of the reaction path by density functional and QCISD(T) calculations strongly suggest that the mechanism of $CH + C_2H_4$ is dominated by addition to the double bond. From the proposed mechanism in Figure 6, the kinetic isotope effect for the deuteration of the CH radical, i.e. k_{CH}/k_{CD} , in the reaction $CH/CD + \text{pyrrole}$ at room temperature (295 K) and 363 K would also be expected to be negligible.

4.2. Possible implications for Titan and combustion chemistry

A recent photochemical model by Krasnopolsky⁴ stresses the fact that hydrocarbons, nitriles and ion chemistries are strongly coupled on Titan. Because of its unique cold and dense atmosphere, composed primarily of N_2 and several percent of CH_4 ,⁵⁰ and its complex photochemistry, Titan presents analogies to a primitive Earth with prebiotic chemistry⁵¹ and continues to be a fascinating object of our solar system. Continuing analysis of data from direct *in situ* measurements by the Huygens probe⁵² and numerous flybys of the Cassini orbiter continue to significantly unravel the chemical composition of Saturn's moon. Indeed, a great variety of small carbonaceous and nitrogen containing species have been identified,^{50, 53} which most certainly result from ion and/or radical chemistry. Both hydrocarbon and nitrile species, including N-

heterocyclic molecules, are believed to play a central role in the formation of the photochemical haze shrouding Titan.

While the recent identification of benzene⁵³ on Titan strongly suggests that much more complex PAH synthesis⁵⁴ may proceed in the cold photoactive atmosphere, the presence of both pyrrole and pyridine, the simplest 5- and 6-membered N-heterocyclic aromatic molecules, has been indirectly inferred from several laboratory experiments^{14,15} simulating Titan tholins.⁵⁵ In comparison to a PAH homologue, calculations suggest that the inclusion of a nitrogen atom could facilitate ring formation by lowering ring closure barriers.¹⁹ Because it is thought that PAHs are probably the most abundant sources of organic carbon in the Interstellar Medium (ISM),⁵⁶ it could also be argued that the presence of N atoms in such polycyclic aromatics could eventually favor molecular weight growth of much larger N-substituted PAHs.

Likewise, pyridine, compared to benzene, has a large proton affinity, which implies efficient proton transfer reactions as suggested in a recent study by Fondren and coworkers.⁵⁷ The authors observed induced fragmentation of the ring molecule by proton transfer and identified $C_4H_4^+$ and HCN as the main fragments with ions at higher recombination energies.⁵⁷ From their observations, the authors suggest that pyridine could be synthesized in the gas phase through the association reaction involving these two fragments. This ion-molecule reaction could play a significant role as a source of pyridine, given the fact that HCN is particularly stable and abundant in Titan's ionosphere. Note that the radical-molecule $C_3N + C_2H_6$ reaction is the one and only source of C_5H_5N in the model by Krasnopolsky.⁴

Small hydrocarbon radical species like CH and C_2H have been detected on Titan as well as the CN radical. These radical species are involved in a photochemical network with small molecules, e.g. C_2H_2 , C_2H_4 , C_2H_6 or HCN, producing larger complex molecules. Identification of small polyatomic species is comparatively straightforward because of their abundances, the wealth of spectroscopic data and the utilization of high-level *ab initio* calculations. However, it is less obvious to identify larger chain and cyclic molecules due to the numerous possible isomers and multiple reaction pathways.¹⁸ This situation renders interpretation of data collected by the Cassini Ion and Neutral Mass Spectrometer (INMS) more difficult for larger masses.⁵⁰ In that respect,

both kinetic and product detection studies, with isomeric specificity, are central to the identification of chemical pathways and determination of branching fractions in order to assess their relative importance to the formation of higher molecular weight species.

Our motivation to investigate the title reaction is not only based on the astrobiological importance of small N-bearing aromatic molecules but also from a fundamental point of view to examine the possibility of ring expansion reactions. Our product detection experiment demonstrates that the reaction of CH with pyrrole in the gas phase produces pyridine as the primary product through a ring expansion mechanism. Extrapolation of reaction mechanisms down to lower temperatures, such as in Titan's atmosphere, has the potential to be problematic, especially if the entrance channel is temperature sensitive. However, as a general trend, reactions with CH occur with rates close to the capture limit and have a negative temperature dependence. This behavior is consistent with a barrierless reaction where the rate limiting step is the formation of the adduct.⁴⁹ Therefore, even at lower temperatures encountered in the ISM or in the atmosphere of Titan, the cycloaddition of CH radicals to the π -system of pyrrole could lead to ring expansion and formation of the pyridine molecule through H atom loss. Also, the C₅H₅N isomer distribution might be temperature dependent. This result would imply a different molecular structure from the most stable 6-membered ring, for instance linear isomers. However, it could be argued that such a pathway would most probably involve a barrier to ring opening, which might favor the resonance-stabilized cyclic structure.

Because of the presence of CH radicals in combustion, the title reaction could play a role in converting gas-phase pyrrole molecules into pyridine, which are species involved in the combustion of coal and coal-derived fuels. For complete combustion processes, the ultimate fate of such aromatic "nitrogen fuel" is conversion into HCN molecules, partially responsible for the emission of NO.²⁰ However, incomplete combustion leads to the formation of soot particles, which is acknowledged to be another source of environmental pollution. The formation of these particles involves the construction of PAH "seeds" where N-heterocyclic aromatic species such as pyrrole and pyridine could most certainly have an important role to play.

5. Conclusion

The gas-phase reaction of the methylidyne radical (CH) with pyrrole ($\text{C}_4\text{H}_5\text{N}$) has been studied in a slow flow reactor coupled to tunable VUV synchrotron at room temperature (295 K) and 90 °C (363 K), at 4 Torr (533 Pa). The Photoionization Efficiency curve of $m/z = 79$ ion signal identifies pyridine ($\text{C}_5\text{H}_5\text{N}$) as the primary product of the reaction. With deuterated methylidyne (CD), the product mass peak is shifted by +1 mass unit and no evidence of hydrogen randomization was found. In light of these results, a ring expansion mechanism has been proposed, which proceeds *via* the direct CH (CD) cycloaddition or insertion into the five-member pyrrole ring. Consequences for the photochemistry of Titan and combustion flame chemistry have also been indicated.

Acknowledgement

The support of personnel (S.S.) for this research by the National Aeronautics and Space Administration (Grant No. NNX09AB60G) is gratefully acknowledged. We thank Mr. Howard Johnsen for excellent technical support. Sandia authors and instrumentation for this work are supported by the Division of Chemical Sciences, Geosciences and Biosciences, the Office of Basic Energy Sciences, the U.S. Department of Energy. Sandia is a multiprogram laboratory operated by Sandia Corporation, a Lockheed Martin Company, for the National Nuclear Security Administration under Contract No. DE-AC04-94-AL85000. The Advanced Light Source and Chemical Sciences Division (K.R.W. and S.R.L.) are supported by the Director, Office of Science, Office of Basic Energy Sciences of the U.S. Department of Energy under Contract No. DE-AC02-05CH11231 at the Lawrence Berkeley National Laboratory. A.J.T. acknowledges travel funding provided by the International Synchrotron Access Program (ISAP) managed by the Australian Synchrotron. The ISAP is funded by a National Collaborative Research Infrastructure Strategy grant provided by the Federal Government of Australia.

Bibliography

1. J. A. Miller and C. T. Bowman, *Progress in Energy and Combustion Science*, 1989, **15**, 287-338.
2. J. A. Miller, R. J. Kee and C. K. Westbrook, *Annual Review of Physical Chemistry*, 1990, **41**, 345-387.
3. R. A. Brownsword, I. R. Sims, I. W. M. Smith, D. W. A. Stewart, A. Canosa and B. R. Rowe, *Astrophysical Journal*, 1997, **485**, 195-202.
4. V. A. Krasnopolsky, *Icarus*, 2009, **201**, 226-256.
5. F. Goulay, A. J. Trevitt, G. Meloni, T. M. Selby, D. L. Osborn, C. A. Taatjes, L. Vereecken and S. R. Leone, *Journal of the American Chemical Society*, 2009, **131**, 993-1005.
6. M. R. Berman and M. C. Lin, *Chemical Physics*, 1983, **82**, 435-442.
7. H. Thiesemann, J. MacNamara and C. A. Taatjes, *Journal of Physical Chemistry A*, 1997, **101**, 1881-1886.
8. F. Goulay, C. Rebrion-Rowe, L. Biennier, S. D. Le Picard, A. Canosa and B. R. Rowe, *Journal of Physical Chemistry A*, 2006, **110**, 3132-3137.
9. J. C. Loison and A. Bergeat, *Physical Chemistry Chemical Physics*, 2009, **11**, 655-664.
10. K. McKee, M. A. Blitz, K. J. Hughes, M. J. Pilling, H. B. Qian, A. Taylor and P. W. Seakins, *Journal of Physical Chemistry A*, 2003, **107**, 5710-5716.
11. D. G. Johnson, M. A. Blitz and P. W. Seakins, *Physical Chemistry Chemical Physics*, 2000, **2**, 2549-2553.
12. S. B. Charnley, Y. J. Kuan, H. C. Huang, O. Botta, H. M. Butner, N. Cox, D. Despois, P. Ehrenfreund, Z. Kisiel, Y. Y. Lee, A. J. Markwick, Z. Peeters and S. D. Rodgers, 2005.
13. F. Raulin, *Space Sci. Rev.*, 2008, **135**, 37-48.
14. H. Imanaka, B. N. Khare, J. E. Elsila, E. L. O. Bakes, C. P. McKay, D. P. Cruikshank, S. Sugita, T. Matsui and R. N. Zare, *Icarus*, 2004, **168**, 344-366.
15. C. D. Neish, A. Somogyi, J. I. Lunine and M. A. Smith, *Icarus*, 2009, **201**, 412-421.
16. B. N. Khare, C. Sagan, J. E. Zumberge, D. S. Sklarew and B. Nagy, *Icarus*, 1981, **48**, 290-297.
17. E. H. Wilson and S. K. Atreya, *Planetary and Space Science*, 2003, **51**, 1017-1033.
18. D. E. Woon and J. Y. Park, *Icarus*, 2009, **202**, 642-655.
19. A. Ricca, C. W. Bauschlicher and E. L. O. Bakes, *Icarus*, 2001, **154**, 516-521.
20. W. D. James, W. D. Ehmann, C. E. Hamrin and L. L. Chyi, *Journal of Radioanalytical Chemistry*, 1976, **32**, 195-205.
21. L. L. Baxter, R. E. Mitchell, T. H. Fletcher and R. H. Hurt, *Energy & Fuels*, 1996, **10**, 188-196.
22. D. L. Osborn, P. Zou, H. Johnsen, C. C. Hayden, C. A. Taatjes, V. D. Knyazev, S. W. North, D. S. Peterka, M. Ahmed and S. R. Leone, *Review of Scientific Instruments*, 2008, **79**.
23. I. R. Slagle, F. Yamada and D. Gutman, *Journal of the American Chemical Society*, 1981, **103**, 149-153.
24. F. Goulay, D. L. Osborn, C. A. Taatjes, P. Zou, G. Meloni and S. R. Leone, *Physical Chemistry Chemical Physics*, 2007, **9**, 4291-4300.
25. G. Meloni, T. M. Selby, F. Goulay, S. R. Leone, D. L. Osborn and C. A. Taatjes, *Journal of the American Chemical Society*, 2007, **129**, 14019-14025.

26. A. J. Trevitt, F. Goulay, G. Meloni, D. L. Osborn, C. A. Taatjes and S. R. Leone, *International Journal of Mass Spectrometry*, 2009, **280**, 113-118.
27. P. Zou, J. N. Shu, T. J. Sears, G. E. Hall and S. W. North, *Journal of Physical Chemistry A*, 2004, **108**, 1482-1488.
28. M. H. Palmer, I. C. Walker and M. F. Guest, *Chemical Physics*, 1998, **238**, 179-199.
29. A. J. van den Brom, M. Kapelios, T. N. Kitsopoulos, N. H. Nahler, B. Cronin and M. N. R. Ashfold, *Physical Chemistry Chemical Physics*, 2005, **7**, 892-899.
30. C. Romanzin, S. Boye-Peronne, D. Gauyacq, Y. Benilan, M. C. Gazeau and S. Douin, *Journal of Chemical Physics*, 2006, **125**.
31. F. C. James, B. Ruzsicska, R. S. McDaniel, R. Dickson, O. P. Strausz and T. N. Bell, *Chemical Physics Letters*, 1977, **45**, 449-453.
32. R. S. McDaniel, R. Dickson, F. C. James, O. P. Strausz and T. N. Bell, *Chemical Physics Letters*, 1976, **43**, 130-134.
33. B. P. Ruzsicska, A. Jodhan, H. K. J. Choi, O. P. Strausz and T. N. Bell, *Journal of the American Chemical Society*, 1983, **105**, 2489-2490.
34. A. Canosa, I. R. Sims, D. Travers, I. W. M. Smith and B. R. Rowe, *Astronomy and Astrophysics*, 1997, **323**, 644-651.
35. N. Daugey, P. Caubet, B. Retail, M. Costes, A. Bergeat and G. Dorthé, *Physical Chemistry Chemical Physics*, 2005, **7**, 2921-2927.
36. C. Utsunomiya, T. Kobayashi and S. Nagakura, *Bulletin of the Chemical Society of Japan*, 1978, **51**, 3482-3484.
37. C. J. Emanuel and P. B. Shevlin, *Journal of the American Chemical Society*, 1994, **116**, 5991-5992.
38. N. Balucani, O. Asvany, Y. Osamura, L. C. L. Huang, Y. T. Lee and R. I. Kaiser, *Planetary and Space Science*, 2000, **48**, 447-462.
39. A. Bergeat and J. C. Loison, *Physical Chemistry Chemical Physics*, 2001, **3**, 2038-2042.
40. M. A. Blitz, M. S. Beasley, M. J. Pilling and S. H. Robertson, *Physical Chemistry Chemical Physics*, 2000, **2**, 805-812.
41. J. E. Butler, J. W. Fleming, L. P. Goss and M. C. Lin, *Chemical Physics*, 1981, **56**, 355-365.
42. R. I. Kaiser, O. Asvany and Y. T. Lee, *Planetary and Space Science*, 2000, **48**, 483-492.
43. A. J. Trevitt, F. Goulay, C. A. Taatjes, D. L. Osborn and S. R. Leone, *Journal of Physical Chemistry A*, 2010, **114**, 1749-1755.
44. M. R. Berman, J. W. Fleming, A. B. Harvey and M. C. Lin, *Chemical Physics*, 1982, **73**, 27-33.
45. G. Dupeyrat, J. B. Marquette and B. R. Rowe, *Physics of Fluids*, 1985, **28**, 1273-1279.
46. B. R. Rowe, G. Dupeyrat, J. B. Marquette and P. Gaucherel, *Journal of Chemical Physics*, 1984, **80**, 4915-4921.
47. F. Goulay, C. Rebrion-Rowe, J. L. Le Garrec, S. D. Le Picard, A. Canosa and B. R. Rowe, *Journal of Chemical Physics*, 2005, **122**.
48. C. Barckholtz, T. A. Barckholtz and C. M. Hadad, *Journal of the American Chemical Society*, 1999, **121**, 491-500.
49. H. Thiesemann, E. P. Clifford, C. A. Taatjes and S. J. Klippenstein, *Journal of Physical Chemistry A*, 2001, **105**, 5393-5401.
50. J. Cui, R. V. Yelle, V. Vuitton, J. H. Waite, W. T. Kasprzak, D. A. Gell, H. B. Niemann, I. C. F. Muller-Wodarg, N. Borggren, G. G. Fletcher, E. L. Patrick, E. Raaen and B. A. Magee, *Icarus*, 2008, **200**, 581-615.

51. F. Raulin, 2005.
52. J. P. Lebreton, A. Coustenis, J. Lunine, F. Raulin, T. Owen and D. Strobel, *Astron. Astrophys. Rev.*, 2009, **17**, 149-179.
53. A. Coustenis, R. K. Achterberg, B. J. Conrath, D. E. Jennings, A. Marten, D. Gautier, C. A. Nixon, F. M. Flasar, N. A. Teanby, B. Bezard, R. E. Samuelson, R. C. Carlson, E. Lellouch, G. L. Bjoraker, P. N. Romani, F. W. Taylor, P. G. J. Irwin, T. Fouchet, A. Hubert, G. S. Orton, V. G. Kunde, S. Vinatier, J. Mondellini, M. M. Abbas and R. Courtin, *Icarus*, 2007, **189**, 35-62.
54. A. M. Mebel, V. V. Kislov and R. I. Kaiser, *Journal of the American Chemical Society*, 2008, **130**, 13618-13629.
55. M. G. Tomasko, B. Archinal, T. Becker, B. Bezard, M. Bushroe, M. Combes, D. Cook, A. Coustenis, C. de Bergh, L. E. Dafoe, L. Doose, S. Doute, A. Eibl, S. Engel, F. Gliem, B. Grieger, K. Holso, E. Howington-Kraus, E. Karkoschka, H. U. Keller, R. Kirk, R. Kramm, M. Kuppers, P. Lanagan, E. Lellouch, M. Lemmon, J. Lunine, E. McFarlane, J. Moores, G. M. Prout, B. Rizk, M. Rosiek, P. Rueffer, S. E. Schroder, B. Schmitt, C. See, P. Smith, L. Soderblom, N. Thomas and R. West, *Nature*, 2005, **438**, 765-778.
56. O. Botta, *Proceedings IAU Symposium*, 2005, **231**, 479-488.
57. L. D. Fondren, J. McLain, D. M. Jackson, N. G. Adams and L. M. Babcock, *International Journal of Mass Spectrometry*, 2007, **265**, 60-67.
58. D. A. Blank, S. W. North and Y. T. Lee, *Chemical Physics*, 1994, **187**, 35-47.
59. J. H. Kiefer, Q. Zhang, R. D. Kern, J. Yao and B. Jursic, *Journal of Physical Chemistry A*, 1997, **101**, 7061-7073.

Captions for figures

Figure 1: Molecular structures of some aromatic molecules: (a) pyrrole, (b) pyridine and (c) benzene. The different sites in pyrrole and pyridine are labeled as indicated.

Figure 2: Mass spectra of (a) CH + pyrrole and (b) CD + pyrrole reactions at 10.2 eV photoionization energy. The data is integrated for $0 < t < 50$ ms. The entire mass peak of the product (C_5H_5N) is shifted by +1 mass unit (C_5H_4DN) when CH radicals are replaced by CD radicals in the flow.

Figure 3: Time-resolved mass spectrum of CH + pyrrole reaction at 10.2 eV photoionization energy. The product ($m/z = 79$) can be distinguished from the reactant ($m/z = 67$) as it appears after the laser pulse (indicated by a dashed line at $t = 0$ ms).

Figure 4: Evolution of $m/z = 79$ ion signals as a function of reaction time at (a) 295 K and (b) 363 K. Note that the signal-to-background level, i.e. before the photolysis laser pulse at $t = 0$, is substantially reduced from 295 K to 363 K. The shape of the curve using the heated tube at 363 K reflects the heating profile (see text).

Figure 5: (a) and (b) Energy resolved mass spectra, and (c) and (d) Photoionization Efficiency (PIE) curve of $m/z = 79$ ion signal for CH + pyrrole and $m/z = 80$ ion signal for CD + pyrrole reactions respectively. The signal at $m/z = 79$ in (b) is due to a contamination of $CDBr_3$ with the hydrogenated species (99.5% of D, Sigma Aldrich). The black curve in (c) and (d) is a fit of the experimental data points using a relative PIE curve of pyridine.

Figure 6: Proposed ring expansion mechanism for the title reaction. Step 1 involves the addition of the methyldiylne radical (CH) to a double bond in the heterocyclic 5-membered ring. In step 2, ring opening leads to the insertion of the C atom in the ring to give the allylic stabilized intermediate. Bond rearrangement in step 3 followed by H atom elimination from the nitrogen in step 4 leads to the formation of pyridine. This mechanism implies that the initial carbon atom in the CH radical is located on site 2 (see Figure 1 for label).

Captions for Tables

Table 1: Bond dissociation energies (in kcal/mol) at 298 K: N-H bond in pyrrole and C-H bonds in both pyrrole and pyridine (see Figure 1 for labeling of the carbon atoms).

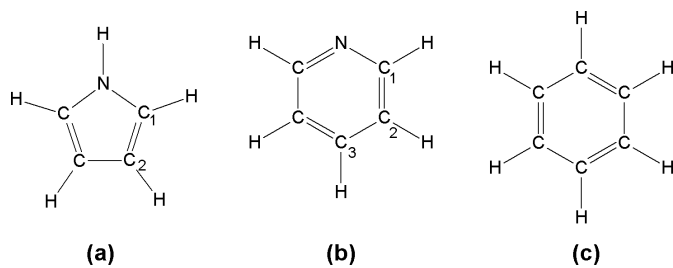


Figure 1

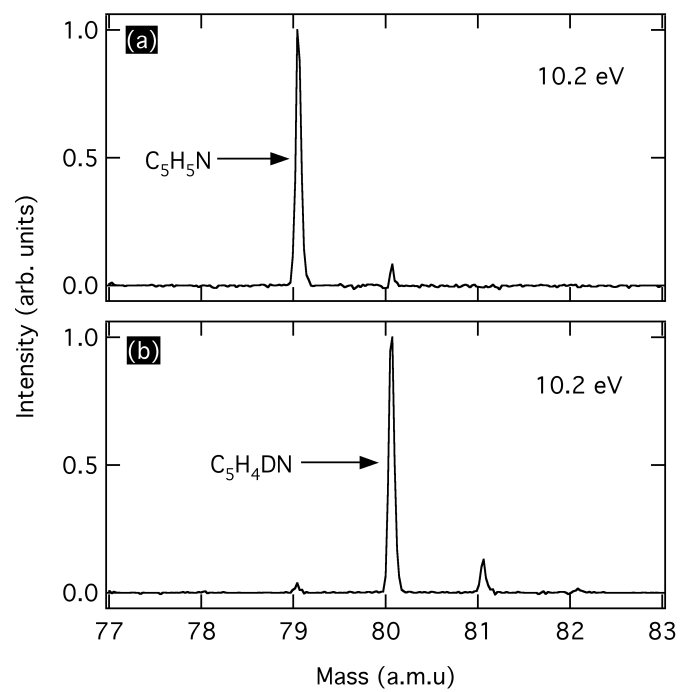


Figure 2

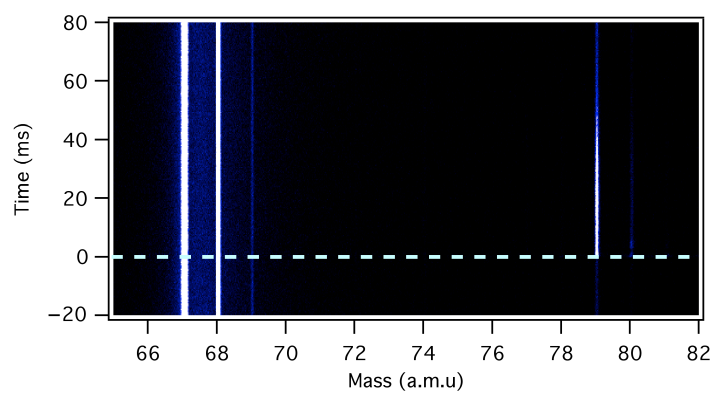


Figure 3

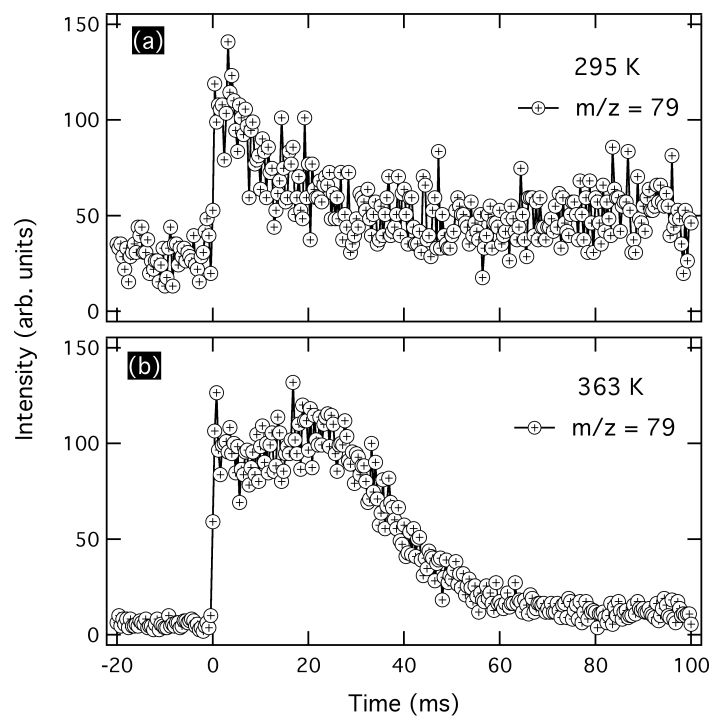


Figure 4

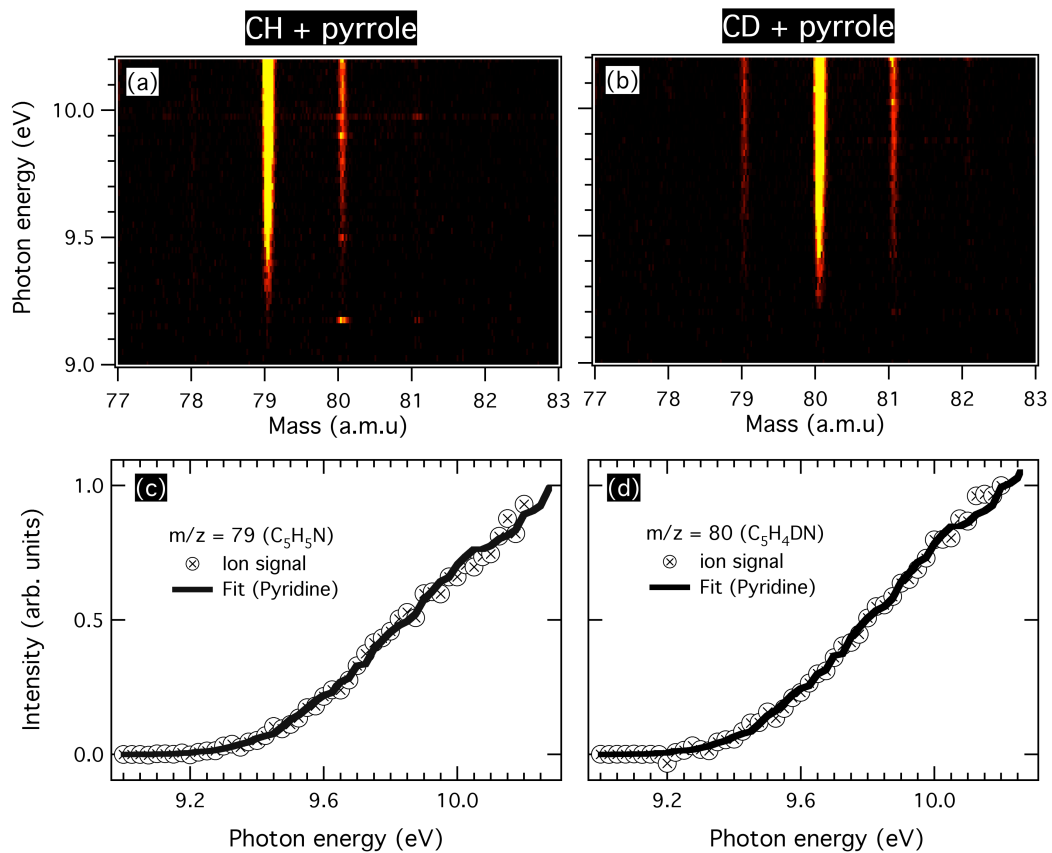


Figure 5

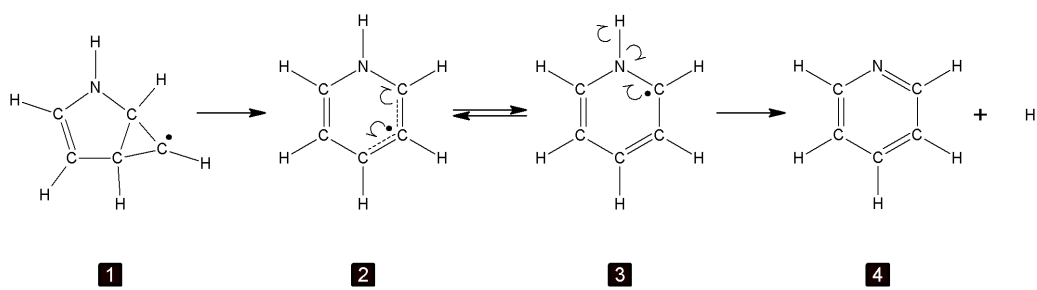


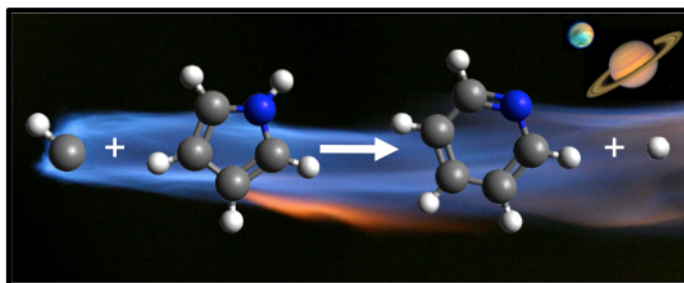
Figure 6

Table 1

Species	Site	B3LYP calculations ^a	Experimental
pyrrole	1	118.1	112.3 ^b
	2	117.6	112.3 ^b
	N	89.8	88 ^b
pyridine	1	105.6	105±2 ^c
	2	111.3	112±2 ^c
	3	110.0	112±2 ^c

^aRef.⁴⁸^bRef.⁵⁸^cRef.⁵⁹

TOC graphic



Direct identification of a ring expansion reaction involving the CH radical with pyrrole leading to the formation of the N-heterocyclic molecule, pyridine.